

Nanoscale imaging of photoelectrons using an atomic force microscope

Ping Yu and Jürgen Kirschner

Citation: *Appl. Phys. Lett.* **102**, 063111 (2013); doi: 10.1063/1.4792270

View online: <http://dx.doi.org/10.1063/1.4792270>

View Table of Contents: <http://apl.aip.org/resource/1/APPLAB/v102/i6>

Published by the [American Institute of Physics](#).

Related Articles

Scattering and the relationship between quantum efficiency and emittance

J. Appl. Phys. **113**, 056101 (2013)

The change of electrical transport characterizations in Ga doped ZnO films with various thicknesses

J. Appl. Phys. **113**, 053702 (2013)

Effective attenuation length for lanthanum lutetium oxide between 7 and 13keV

Appl. Phys. Lett. **102**, 031607 (2013)

Studies of the oxidation states of phosphorus gettered silicon substrates using X-ray photoelectron spectroscopy and transmission electron microscopy

J. Appl. Phys. **113**, 044307 (2013)

Detecting the local transport properties and the dimensionality of transport of epitaxial graphene by a multi-point probe approach

Appl. Phys. Lett. **102**, 033110 (2013)

Additional information on *Appl. Phys. Lett.*

Journal Homepage: <http://apl.aip.org/>

Journal Information: http://apl.aip.org/about/about_the_journal

Top downloads: http://apl.aip.org/features/most_downloaded

Information for Authors: <http://apl.aip.org/authors>

ADVERTISEMENT

AIP | Applied Physics
Letters

SURFACES AND INTERFACES
Focusing on physical, chemical, biological, structural, optical, magnetic and electrical properties of surfaces and interfaces, and more...

ENERGY CONVERSION AND STORAGE
Focusing on all aspects of static and dynamic energy conversion, energy storage, photovoltaics, solar fuels, batteries, capacitors, thermoelectrics, and more...

EXPLORE WHAT'S NEW IN APL

SUBMIT YOUR PAPER NOW!

Nanoscale imaging of photoelectrons using an atomic force microscope

Ping Yu^{a)} and Jürgen Kirschner

Max Planck Institute of Microstructure Physics, Weinberg 2, 06120 Halle, Germany

(Received 30 November 2012; accepted 31 January 2013; published online 13 February 2013)

Photoemission current imaging at the nanoscale is demonstrated by combining an atomic force microscope with laser excitation. Photoelectrons emitted from the sample are collected by the tip while the tip-sample distance is precisely controlled by their van der Waals force interaction. We observe pronounced photoemission current contrast with spatial resolution of 5 nm on a cesium covered Au(111) surface. This high spatial resolution can be attributed to the strong dependence of the local potential barrier on the tip-sample distance. Our experiments provide a method for photoelectron imaging with high spatial resolution and extend the functionality of state-of-the-art scanning probe techniques. © 2013 American Institute of Physics. [<http://dx.doi.org/10.1063/1.4792270>]

Nanotechnology demands advanced methods for investigating the properties of microstructures and surfaces at the nanometer scale. Photoemission electron microscopy (PEEM) as a powerful tool has been extensively applied since the spatial mapping of photoelectrons not only carries information about the electronic properties of materials but also allows identification of chemical^{1,2} as well as magnetic states of systems.^{3,4} Conventionally PEEM requires accurate electron optics to collect photoelectrons and the spatial resolution is strongly limited by varieties of aberrations. With rather involved efforts, the resolution of PEEM can reach around 10 nm.^{5–8}

Compared with electron-optics based PEEM, scanning probe microscopy (SPM) can easily reach sub nanometer spatial resolution. It is, therefore, an interesting issue, whether SPM can be used for photoelectron imaging with high spatial resolution. Considering the narrow acceptance angle of the SPM tip and the small tip-sample distance for collecting electrons, the tip could be an ideal local detector for photoelectron imaging with high spatial resolution. Gimzewski *et al.* first used the tip of a scanning tunneling microscope (STM) to collect photoelectrons.⁹ In their experiments, the photoelectron current was detected by the STM tip 50 nm away from the sample surface and photoelectron imaging with sub-micrometer spatial resolution was demonstrated. Later, Gray and Okuda *et al.* combined STM with intensity modulated laser¹⁰ and synchrotron radiation excitation.^{11,12} The associated modulation of photoelectron current can be separated from the tunneling current by lock-in technique, and the estimated spatial resolution of photoelectron mapping could reach 10 nm.¹² As an alternative, Spanakis *et al.* developed a prototype using an atomic force microscope with a metal-coated microcantilever operated in ambient condition, by which sub-micrometer spatial resolution of photoelectron mapping was shown.¹³

In this letter, we report a method to obtain high spatial resolution of 5 nm in photoemission (PE) current imaging using a Qplus AFM. The idea is based on the observation that there exists a certain distance range between the tip and

the sample where their attractive interaction is still large enough to support a dynamic stabilization of the distance while scanning the surface morphology. Moreover, the tip-sample distance may be chosen large enough to suppress any significant tunneling current. So, our setup realizes a straightforward detection of pure photoelectron current without tunneling contribution and allows an independent control of the tip-sample distance. By precisely varying the gap distance between the tip and the sample, we observe a rapid decay of photoemission current at increasing gap distance. This strong current versus distance dependence provides a mechanism for high resolution photoelectron imaging.

The experimental setup is shown in Fig. 1. We use a fiber laser to excite the tip-sample gap. The laser has an average power of 2 mW centered at 680 nm.¹⁴ After passing through a beam expander (BE), the laser beam is expanded to a diameter of 10 mm and then focused by a lens with focal length of 65 mm in the ultrahigh vacuum chamber. The laser focus has a diameter of 20 μm . We use the Qplus AFM sensor as a local probe which can be operated in either the constant current STM mode or the constant shift frequency AFM mode. The Qplus sensor has a tungsten tip glued on one prong of the tuning fork, which oscillates at a resonance frequency of 24 kHz.¹⁶ During experiments, as the tip

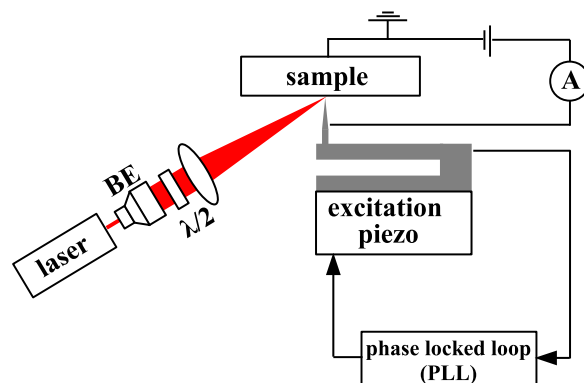


FIG. 1. Geometry of the experimental setup. Using a BE and mounting the lens near to the sample, the laser focus spot is reached to 20 μm . $\lambda/2$ is the half wave plate for setting *p*- or *s*-polarization. The shift frequency provides feedback for the tip-sample distance control while the current flowing between the tip and the sample is measured.

^{a)} Author to whom correspondence should be addressed. Electronic mail: pingyu@mpi-halle.de.

approaches the sample, the resonance frequency of the tuning fork decreases due to the attractive van der Waals force between the tip and the sample. In the intended mode of operation, this frequency shift is used as a feedback for keeping the tip-sample distance at a chosen constant value during scanning over the surface. The photoelectron current flowing within the junction can be detected at the fA level using a current-voltage converter.¹⁵ With this setup, scanning the sample morphology and detecting photoelectrons can be done simultaneously and independently.

We image the photoemission current by the AFM tip on a cesium covered Au(111) surface. The Au(111) sample is cleaned by standard sputtering and annealing procedures. Cs atoms are then deposited from a getter source on the clean Au(111) surface at 300 K. With sub monolayer Cs coverage, the work function of the Au(111) surface decreases below 2 eV because of the dipole layer induced by electron transfer from the Cs layer to the gold surface.^{17,18} Due to the small separation between the tip and the sample, the local barrier for photoelectrons to propagate from the sample to the tip can be strongly influenced by the applied bias voltage. Figure 2(a) shows the topography of Cs/Au(111) surface

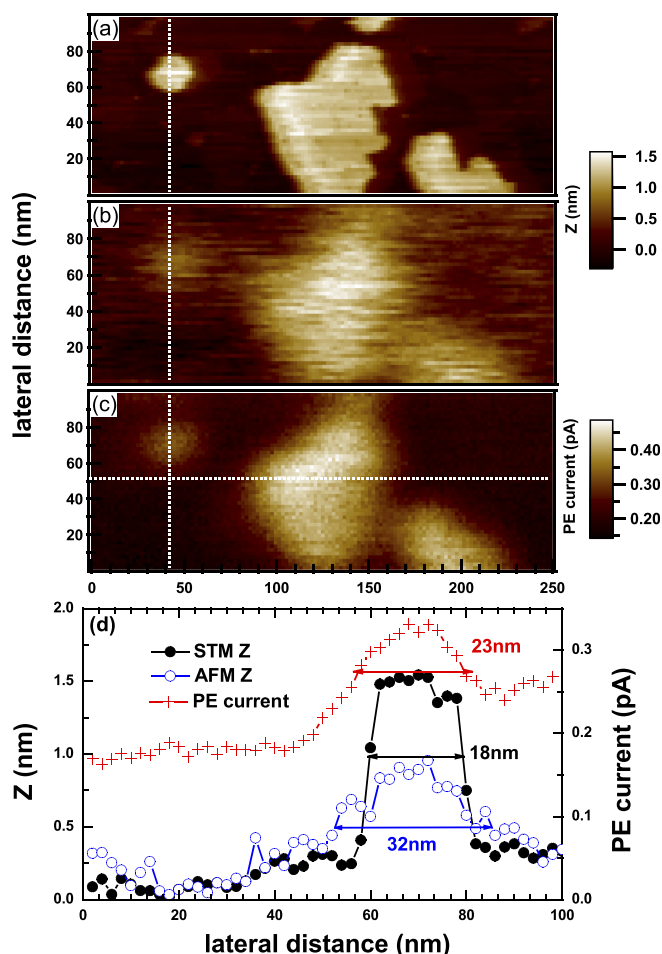


FIG. 2. (a) Topographic image of Cs/Au(111) measured in STM constant current mode ($V_{tip}=0.2$ V, $I_{tunnel}=0.5$ nA). (b) Topography image of Cs/Au(111) measured in AFM mode with -0.5 Hz shift frequency and bias $V_{tip}=+2$ V. (c) PE current image of Cs/Au(111) measured in AFM mode with -0.5 Hz shift frequency. (d) Line profiles of topography measured in STM, AFM, and photoemission current along the vertical dashed lines indicated in (a), (b), and (c).

measured in the STM constant tunneling current mode, revealing the nanoscale islands formed by cesium atoms. Figs. 2(b) and 2(c) are the AFM topography and the corresponding PE current images measured at -0.5 Hz shift frequency and $+2$ V tip bias voltage with laser illumination. Since the whole surface is covered by varying amounts of Cs, we observe a certain level of PE current everywhere and pronounced PE current contrast between Cs islands and terraces underneath. If without laser illumination, only a constant background current of about 150 fA can be detected which is the leakage current by the electronics. Comparing the PE current mapping and the corresponding topography images, we find that the collected photoemission current is about 200 fA higher above the Cs islands than that above the terraces. This contrast mechanism can be attributed to the Cs coverage dependent work function and electronic properties of Cs/Au(111).^{19,20}

Figure 2 clearly shows that the STM topography image has the best spatial resolution, while the PE current image has better resolution than the AFM topography image. To quantitatively estimate the spatial resolution, line profiles along the vertical dotted lines in Figs. 2(a)–2(c) are shown in Fig. 2(d). The full-width-at-half-maximum (FWHM) of the cesium island in STM and AFM topographic line profiles is 18 nm and 32 nm, while the FWHM of the PE current line profile on the same island is 23 nm. By assuming the intrinsic width of the island as 18 nm as measured in the STM line profile, we can estimate the spatial resolution of PE current mapping to be around 5 nm. This value is smaller than the best resolution in PEEM⁸ or in imaging of photoelectrons using a STM tip.¹²

To investigate the origin of this high spatial resolution of PE current imaging, we measure the PE current line profiles along the horizontal dotted line marked in Fig. 2(c) as a function of shift frequency as displayed in Fig. 3(a). During the measurement of PE current line profiles, the tip positions are recorded simultaneously as shown in Fig. 3(b). The grey round symbols in Fig. 3(a) show the background current measured without laser illumination. Under laser illumination, PE current is measured with a shift frequency varying from -0.4 Hz to -1.2 Hz. The hollow circle symbols in Fig. 3(a) represent the PE current measured at -0.4 Hz, which is comparable to the background current since the tip-sample distance is as large as about 40 nm and no surface topography can be imaged with this frequency shift. As shown in Figs. 3(a) and 3(b), the PE current increases as the tip to sample distance is reduced by increasing the magnitude of the frequency shift. As the resonant frequency shifts more than -1.2 Hz, spikes appear in the current line profile, which are due to local tunneling current contributions. The tip-sample distance at the shift frequency of -1.2 Hz is assumed to be 5 nm, which is the estimated minimum gap size without tunneling current.²¹ The tip-sample distance of the other shift frequencies is derived according to the measured tip displacements.

The averaged values of photoemission current on the Cs island and terrace as a function of tip-sample distance are shown in Fig. 4(a). The averaged photoemission current values are obtained from the raw data by subtracting the background current without laser illumination and then averaged

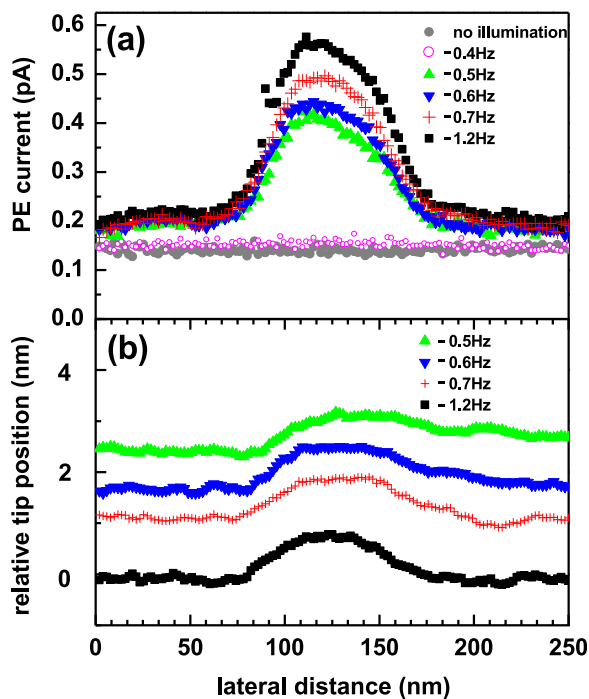


FIG. 3. (a) Photoelectron current line profiles measured along the horizontal dotted line in Fig. 2(c). Symbol round dots represent the current profile without laser illumination. The other line scans are measured with laser illumination at different shift frequencies. (b) Topographic line profiles measured at different shift frequencies.

over the island or the terrace. As shown in Fig. 4(a), the collected photoelectron current decreases rapidly within several nanometers of tip to sample distance.

To explain the dependence of the PE current as a function of the tip-sample distance, we propose a mechanism shown in Fig. 4(b). At small tip to sample distance, the local energy barrier for photoelectrons to transport from the sample to the tip can be reduced by the image potential and by the applied electric field.^{22,23} Since the electric field decreases with increasing tip-sample distance, the PE current will decrease with increasing the gap distance. Guth and

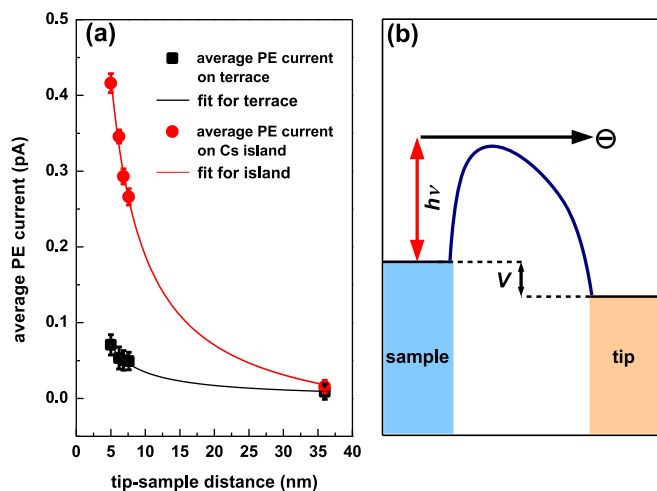


FIG. 4. (a) Averaged photoemission currents of Cs island and terrace as a function of tip-sample distance. The lines are the fitting with the distance by a function $f(x) = P_1 + P_2/x$. For terrace, $P_1 = -0.5$ fA, $P_2 = 352$ fA/nm, while for island $P_1 = -47$ fA, $P_2 = 2361$ fA/nm. (b) Schematic drawing of the local barrier reduction by image potential and electric field.

Mullin showed that as the strength of the static electric field is above 10^4 V/cm and the incident photon energy is close to the photoemission threshold, the photoemission current is mainly proportional to the magnitude of the electric field.²⁴ In our experiment, the incident photon energy 1.83 eV is close to the photoemission threshold and the applied electric field is larger than 10^6 V/cm. According to the theory of Guth and Mullin, the photoemission current should be proportional to the magnitude of the electric field and consequently reciprocal to the tip-sample distance. In Fig. 4(a), the experimental data points are fitted by a $f(x) = P_1 + P_2/x$ function and show reasonable agreement. The parameter P_2 for the island is about 7 times larger than the value for the terrace, indicating the PE current decay rate with the tip-sample distance above Cs island is larger than that on the terrace.

Due to the barrier reduction by the electric field, the photoemission current is proportional to the magnitude of the electric field. However, the electric field at the surface is extremely large just under the tip, but decays rapidly with increasing radial distance from the tip within one tip radius (several nanometers).²⁵ So, the surface barrier is reduced locally only below the tip apex by the applied tip voltage. In this case, only the local area below the tip apex will contribute to the PE current signal dominantly. This explains qualitatively the high spatial resolution in photoemission current mapping.

To summarize, we demonstrate local mapping of photoelectrons using an atomic force microscope. Our setup allows straightforward separation of the photoelectron current from the tunneling current and an independent control of the distance between the tip and the sample. By precisely varying the tip-sample distance, we observe a reciprocal dependence of photoelectron current as a function of the tip-sample separation. This dependence is attributed to the local barrier reduction by the applied electric field between the tip and the sample which provides a mechanism for the observed high spatial resolution of 5 nm. Comparing with the ordinary local work function measurements such as photoemission electron microscopy with several tens of nanometer resolution, Kelvin probe force microscopy with nanometer resolution, and local barrier mapping by STM with the atomic resolution,^{26,27} the resolution of our method is mainly determined by the tip-sample distance which is intendedly controlled at several nanometers to suppress the tunneling current. The main advantage of our method is that we obtain the pure photoemission current mapping with nanometer resolution which represents not only the local work function distribution but also the joint electronic states involved in the photoemission process. So, the local work function and the properties of electronic states can both be measured using our method. For example, the local electronic states contributing to the photoemission can be detected by measuring the local photoelectron spectroscopy with sweeping the photon energy. The photoemission current mapping contrast can be tuned by changing the photon energy for exciting the different electronic states or tuned by changing the laser polarization for the photoemission selection rules. The magnetic nanostructures can also be the target for the future experiment by detecting the photoemission

current mapping difference between left and right circular polarization of illumination. So, our results extend the functionality of scanning probe microscopy in combination with laser excitation and may be widely applied to investigate the electronic properties of nanostructured materials under the optical excitation.

- ¹E. Bauer, M. Munschau, W. Sweich, and W. Telieps, *Ultramicroscopy* **31**, 49–57 (1989).
- ²M. Escher, N. Weber, M. Merkel, C. Ziethen, P. Bernhard, G. Schönhense, S. Schmidt, F. Forster, F. Reinert, B. Krömker, and D. Funnemann, *J. Phys.: Condens. Matter* **17**, S1329 (2005).
- ³J. Stöhr, Y. Wu, B. D. Hermsmeier, M. G. Samant, G. R. Harp, S. Koranda, D. Dunham, and B. P. Tonner, *Science* **259**, 658 (1993).
- ⁴W. Kuch, R. Frmter, J. Gilles, D. Hartmann, Ch. Ziethen, C. M. Schneider, G. Schönhense, W. Swiech, and J. Kirschner, *Surf. Rev. Lett.* **5**, 1241 (1998).
- ⁵P. E. Batson, N. Dellby, and O. L. Krivanek, *Nature* **418**, 617 (2002).
- ⁶P. Schmid, J. Feng, H. Padmore, D. Robin, H. Rose, R. Schlueter, W. Wan, E. Forest, and Y. Wu, *Rev. Sci. Instrum.* **76**, 023302 (2005).
- ⁷B. H. Frazer, M. Girasole, L. M. Wiese, T. Franz, and G. D. Stasio, *Ultramicroscopy* **99**, 87 (2004).
- ⁸F. Kronast, N. Friedenberger, K. Ollefs, S. Gliga, L. Tati-Bismaths, R. Thies, A. Ney, R. Weber, C. Hassel, F. M. Römer, A. V. Trunova, C. Wirtz, R. Hertel, H. A. Dürr, and M. Farle, *Nano Lett.* **11**, 1710 (2011).
- ⁹J. K. Gimzewski, R. Berndt, and R. R. Schlittler, *Ultramicroscopy* **42–44**, 366 (1992).
- ¹⁰S. M. Gray, *J. Electron Spectrosc. Relat. Phenom.* **109**, 183 (2000).
- ¹¹T. Eguchi, T. Okuda, T. Matsushima, A. Kataoka, A. Harasawa, K. Akiyama, T. Kinoshita, Y. Hasegawa, M. Kawamori, Y. Haruyama, and S. Matsui, *Appl. Phys. Lett.* **89**, 243119 (2006).
- ¹²T. Okuda, T. Eguchi, K. Akiyama, A. Harasawa, T. Kinoshita, Y. Hasegawa, M. Kawamori, Y. Haruyama, and S. Matsui, *Phys. Rev. Lett.* **102**, 105503 (2009).
- ¹³E. Spanakis, A. Chimmalgi, E. Stratakis, C. P. Grigoropoulos, C. Fotakis, and P. Tzanetakisa, *Appl. Phys. Lett.* **89**, 013110 (2006).
- ¹⁴Fianium ultrafast fiber laser SC400-PP-AOTF, Fianium Ltd., Unit 20 Compass Point, Hamble, Southampton, UK.
- ¹⁵VT SPM, Omicron Nanotechnology GmbH, Germany.
- ¹⁶F. J. Giessible, *Appl. Phys. Lett.* **76**, 1470 (2000).
- ¹⁷G. S. Leatherman and R. D. Diehl, *Phys. Rev. B* **53**, 4939 (1996).
- ¹⁸M. Caragiu, G. S. Leatherman, R. D. Diehl, P. Kaukasoina, and M. Lindroos, *Surf. Sci.* **441**, 84 (1999).
- ¹⁹S. H. Chou, J. Voss, I. Bargatin, A. Vojvodic, R. T. Howe, and F. A. Pedersen, *J. Phys.: Condens. Matter* **24**, 445007 (2012).
- ²⁰P. Yu and J. Kirschner, “Tip enhanced nanoscale photoelectron imaging and spectroscopy” (unpublished).
- ²¹R. G. Lerner and G. L. Trigg, *Encyclopedia of Physics*, 2nd ed. (VCH, 1991), p. 1308.
- ²²E. O. Lawrence and L. B. Linford, *Phys. Rev.* **36**, 482 (1930).
- ²³W. S. Huxford, *Phys. Rev.* **38**, 379 (1931).
- ²⁴E. Guth and C. J. Mullin, *Phys. Rev.* **59**, 867 (1941).
- ²⁵L. J. Whitman, J. A. Stroschio, R. A. Dragoset, and R. J. Celotta, *Science* **251**, 1206 (1991).
- ²⁶W. Melitz, J. Shen, A. C. Kummela, and S. Lee, *Surf. Sci. Rep.* **66**, 1 (2011).
- ²⁷Y. Yamada, A. Sinsarp, M. Sasaki, and S. Yamamoto, *Jpn. J. Appl. Phys., Part 1* **41**, 7501 (2002).